QUANTUM OPTICS

Observation of a non-Hermitian phase transition in an optical quantum gas

Fahri Emre Öztürk[1], Tim Lappe[2], Göran Hellmann[1], Julian Schmitt[1]*, Jan Klaers[1]†, Frank Vewinger[1], Johann Kroha[2], Martin Weitz[1]*

Quantum gases of light, such as photon or polariton condensates in optical microcavities, are collective quantum systems enabling a tailoring of dissipation from, for example, cavity loss. This characteristic makes them a tool to study dissipative phases, an emerging subject in quantum many-body physics. We experimentally demonstrate a non-Hermitian phase transition of a photon Bose-Einstein condensate to a dissipative phase characterized by a biexponential decay of the condensate's second-order coherence. The phase transition occurs because of the emergence of an exceptional point in the quantum gas. Although Bose-Einstein condensation is usually connected to lasing by a smooth crossover, the observed phase transition separates the biexponential phase from both lasing and an intermediate, oscillatory condensate regime. Our approach can be used to study a wide class of dissipative quantum phases in topological or lattice systems.

Creating and understanding phases of systems that are dissipatively coupled to the environment is of importance in research fields ranging from optics to biophysics (*1*–*6*). One intriguing aspect of this openness is the possible existence of quantum states that are not otherwise accessible (*7*–*10*). Near-equilibrium physics (*11*, *12*) has been studied in optical quantum gases (*13*), such as photons or polaritons (strongly coupled, mixed states of light and matter), despite their driven-dissipative nature. In particular, Bose-Einstein condensates of photons, realized in dye-filled microcavities by multiple photon absorption and reemission cycles, provide a platform to study quantum dynamics in an open, grand canonical situation where the condensate particles are coupled to a reservoir of the photoexcitable dye molecules (*14*). Photon condensates have the macroscopic mode occupation in common with lasers, but they operate near thermal equilibrium, in distinct contrast to lasers. Naïvely, a smooth crossover between lasing and condensation might be expected given that both phenomena exhibit spontaneous symmetry breaking (*8*, *15*).

Recently, oscillatory dynamics in open dye microcavity systems have been observed (*6*, *16*), a phenomenon that at large resonator losses crosses over to the relaxation oscillations known in laser physics. Unlike in a laser, the stochastic driving induced by grand canonical condensate fluctuations makes the system dynamics observable in stationary-state operation, which characterize the system's state by its second-order coherence. In contrast to closed systems governed by time-reversal symmetric—i.e., Hermitian—dynamics, the dissipative coupling to the environment is described by a non-Hermitian time-evolution operator with complex eigenvalues. Of special interest are exceptional points, where the eigenvalues and the corresponding eigenmodes coalesce (*1*, *17*–*20*). Such points are well known to enable phase transitions (*21*); a first-order phase transition between a photon laser and a polariton condensate has recently been proposed (*8*, *22*).

[1]Institut für Angewandte Physik, Universität Bonn, Wegelerstr. 8, 53115 Bonn, Germany. [2]Physikalisches Institut, Universität Bonn, Nussallee 12, 53115 Bonn, Germany.
*Corresponding author. Email: schmitt@iap.uni-bonn.de (J.S.); martin.weitz@uni-bonn.de (M.W.)
†Present address: Complex Photonic Systems (COPS), MESA+ Institute for Nanotechnology, University of Twente, Drienerlolaan 5, 7522 NB Enschede, Netherlands.

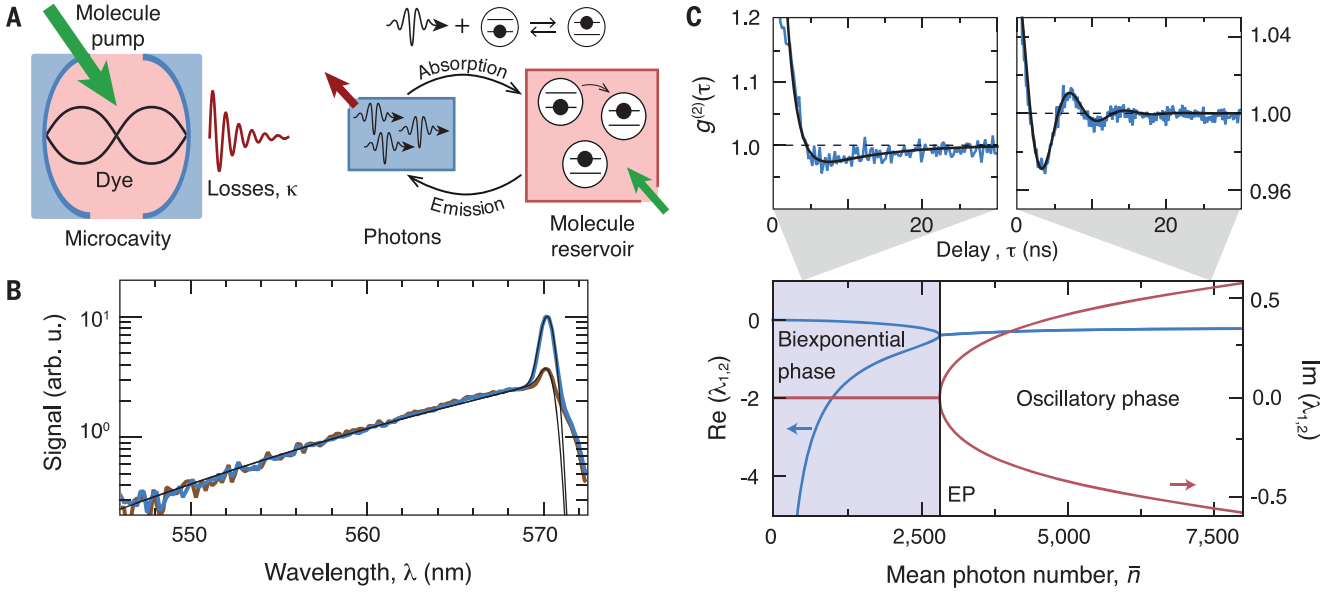

Fig. 1. Experimental principle. (**A**) Photons are trapped within a dye-filled microcavity, where losses κ are compensated by pumping the dye molecules with a laser. The photon gas is coupled to this reservoir by the exchange of excitations between photons and electronically excited dye molecules (right panel). (**B**) Spectra of the emission for average photon numbers $\bar{n} \cong 2100$ (orange line) and 10,300 (blue line), showing a thermalized photon gas with a condensate peak at the position of the low-energy cutoff, closely following the expected (experimentally broadened) Bose-Einstein distributions at 300 K (black lines). arb. u., arbitrary units. (**C**) Second-order correlations $g^{(2)}(\tau)$ of the condensate, recorded at $\bar{n} \cong 2300$ (left) and $\bar{n} \cong 14{,}000$ (right), respectively, with fitted theory curves (black lines) (*25*), showing oscillatory behavior for large photon numbers and a biexponential decay for small photon numbers. The bottom panel shows predictions of real (blue) and imaginary (red) parts of the eigenvalues $\lambda_{1,2}$ (for a molecule number $M = 5 \times 10^9$), which are real below the exceptional point (EP) and complex above it.

To prepare an open photon Bose-Einstein condensate coupled to a reservoir, we use a dye microcavity apparatus (*11*, *23*–*25*) (Fig. 1A). The short mirror spacing of a few wavelengths discretizes the longitudinal wave vector, such that only modes with a fixed longitudinal mode number are accessible to the photon gas at room temperature. This imposes a quadratic dispersion as a function of the transverse wave numbers, and the photon gas becomes formally equivalent to a harmonically trapped two-dimensional gas of massive bosons, which supports Bose-Einstein condensation (*25*). Photons are injected by pumping with a laser beam. They thermalize to the dye temperature by absorption-reemission cycles before being lost by, for example, mirror transmission (Fig. 1A, right panel). The rhodamine dye fulfills the Kennard-Stepanov relation $B_{em}/B_{abs} \propto e^{-\hbar\omega/k_B T}$, a Boltzmann-type frequency scaling between the Einstein coefficients for absorption B_{abs} and emission B_{em}. Experimental spectra show agreement with an equilibrium Bose-Einstein distribution within experimental accuracy (Fig. 1B).

The steady-state particle flux from the pump beam through the dye microcavity condensate and out to the environment induces a modified behavior of the particle number fluctuations. In this open system, the sum X of the condensate photon number $n(t)$ and dye molecular excitations $M_e(t)$ is conserved only on average (*14*, *25*), $\bar{X} = \bar{n} + \bar{M}_e$ is constant, where the bar denotes the time average. The dynamics of the corresponding fluctuations Δn and ΔX around the mean can be derived from a Lindblad equation that incorporates the thermally driven fluctuations of the grand canonical system (equivalent to a Langevin equation). For small deviations Δn and ΔX, this leads to a set of equations (*25*)

$$\frac{d}{dt}\begin{pmatrix}\Delta n \\ \Delta X\end{pmatrix} = \hat{A}\begin{pmatrix}\Delta n \\ \Delta X\end{pmatrix} \quad (1)$$

with the non-Hermitian matrix

$$\hat{A} = \begin{pmatrix}-2\delta & \omega_0^2/\kappa \\ -\kappa & 0\end{pmatrix} \quad (2)$$

where $\delta = \frac{1}{2}B_{em}(\bar{M}_e/\bar{n} + \bar{n})$ is the damping rate of the photon number fluctuations, $\omega_0 = \sqrt{\kappa B_{em}\bar{n}}$ is an oscillation frequency, and the rate constant κ models photon loss. It is instructive to first discuss the expected response to an instantaneous fluctuation at a time t_0. With the exponential ansatz $(\Delta n_0, \Delta X_0) \cdot e^{\lambda(t-t_0)}$, one obtains solutions characterized by the matrix eigenvalues $\lambda_{1,2} = -\delta \pm \sqrt{\delta^2 - \omega_0^2}$. For a damping δ below the natural angular frequency ω_0 of the undamped system, the eigenvalues become complex, corresponding to a (damped) oscillatory solution, while in the opposite regime of a large damping ($\delta > \omega_0$) we arrive at real eigenvalues, implying a biexponential decay. At $\delta = \omega_0$, the eigenvalues and the corresponding solutions coalesce, marking an exceptional point. For stationary conditions, i.e., constant pumping and loss, the dynamics of the grand canonical system driven by thermal fluctuations become stochastic; the modes described above can thus only be observed in the number correlations of the condensate mode, described by $g^{(2)}(\tau) = 1 + e^{-\delta\tau}\left(C_1 e^{-\sqrt{\delta^2-\omega_0^2}\tau} + C_2 e^{\sqrt{\delta^2-\omega_0^2}\tau} + \text{c.c.}\right)$, with constants C_1 and C_2 (c.c., complex conjugate) (*25*).

Tuning between the different regimes—damped oscillatory for $\delta < \omega_0$ and biexponentially decaying correlations for the opposite case—is experimentally achieved by varying the average photon number $\bar{n}$, which with

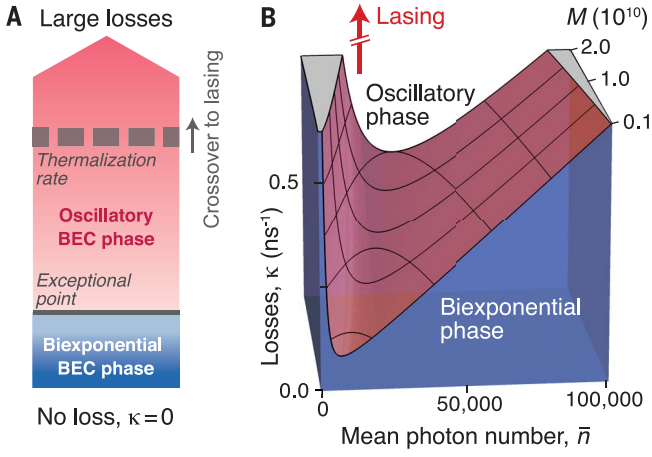

Fig. 2. Expected phase diagram. (**A**) Illustration of the hierarchy of phases for increasing losses, with fixed condensate size and molecule number. The exceptional point introduces a well-defined phase boundary between photon Bose-Einstein condensates with weakly dissipative (biexponential) and dissipative (oscillatory) correlation dynamics. At loss rates exceeding the thermalization rate, a crossover connects the oscillatory phase to the lasing regime. BEC, Bose-Einstein condensate. (**B**) Calculated phase boundary ($\delta = \omega_0$) between the two condensate phases (*25*), as a function of mean condensate and molecule numbers.

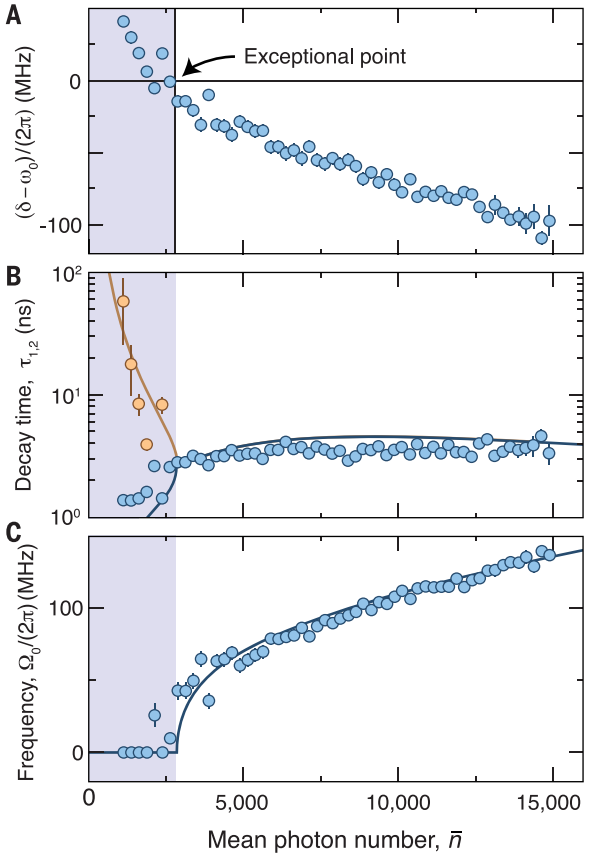

Fig. 3. Non-Hermitian phase transition. (**A**) Variation of the difference $\delta - \omega_0$, (**B**) the decay times, and (**C**) the oscillation frequency with average photon number, determined from the correlation data. Negative (positive) values of $\delta - \omega_0$ (A) indicate an oscillatory (biexponential, blue shading) coherence function. With increasing condensate size, the two decay times (B) merge toward a single value near a photon number $\bar{n}_{EP} \cong 2800$, which displays the phase transition expected from $\delta - \omega_0 = 0$ in (A). Accordingly, above $\bar{n}_{EP}$ the oscillation frequency becomes nonvanishing. The fits yield $\kappa \cong 2.2(2)$ ns^{-1}, $M \cong 4.76(3) \times 10^9$. Error bars are calculated from the uncertainties of the fit parameters. (Cutoff wavelength $\lambda_c = 571.3$ nm).

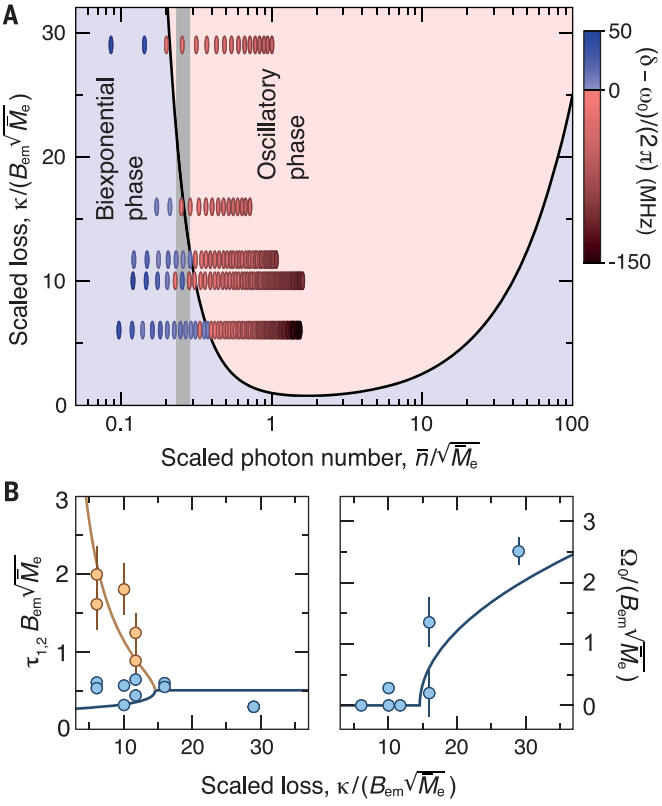

Fig. 4. Exploring the phase diagram. (**A**) The phase boundary between the two regimes (black line) is mapped out by recording different datasets with different cutoff wavelengths and dye concentrations. From the corresponding coherence functions (as in Fig. 3), we identify a condensate in the biexponential (blue points) or oscillatory (red points) phase, respectively. (**B**) Variation of the normalized decay times (left) and oscillation frequency (right) with loss for a scaled photon number $\bar{n}/\sqrt{\bar{M}_e} = 0.27(2)$ [gray shaded area in (A)], showing the transition into the biexponential phase when reducing losses, in good agreement with theory (solid lines). Error bars are calculated from the uncertainties of the fit parameters.

$\omega_0 = \omega_0(\bar{n})$ and $\delta = \delta(\bar{n})$ serves as a control parameter. For small variations of $\bar{n}$, the photon condensate will remain in the oscillatory or the biexponential regime when being far from the exceptional point ($\delta \ll \omega_0$ or $\delta \gg \omega_0$). At the exceptional point ($\delta = \omega_0$), however, the condensate dynamics, as observed in $g^{(2)}(\tau)$, become very sensitive to changes in $\bar{n}$ and may qualitatively change abruptly. We attribute the exceptional point as marking a non-Hermitian phase transition, separating two dynamical condensate phases. The phase transition mechanism draws analogies with that of quantum phase transitions in closed systems, where typically two energy eigenvalues cross; see also (*26*) for a proposal of a dissipative phase transition more closely resembling that of (usual) Hermitian systems. For our system, deep in one of the two condensate phases, the eigenvalues of the fluctuation matrix $A(\bar{n})$ are gapped in the complex plane, and we have $\mathrm{Re}(\lambda_1 - \lambda_2) \neq 0$ or $\mathrm{Im}(\lambda_1 - \lambda_2) \neq 0$ on different sides the transition respectively (Re, real; Im, imaginary; see Fig. 1C, bottom panel). The gap closes ($\lambda_1 = \lambda_2$) at the exceptional point. Notably, critical fluctuations known from equilibrium phase transitions are here replaced by an enhanced sensitivity in the correlation dynamics to changes of the control parameter at the phase boundary. No spontaneous symmetry breaking occurs, which is a property shared with, for example, the fermionic Mott-Hubbard transition. Thermal, reservoir-induced fluctuations of the photon condensate are crucial for the emergence of the described non-Hermitian phase transition.

To experimentally determine the second-order coherence of the photon condensate around the exceptional point, the microcavity emission passes a mode filter to separate the condensate mode from the higher transverse modes. The transmitted light is polarized and directed onto a fast photomultiplier, whose electronic output allows for correlation analysis. Typical obtained traces of the second-order correlations are shown for a cutoff wavelength $\lambda_c \cong 571.3$ nm (Fig. 1C). Whereas for the larger condensate photon number of $\bar{n} \cong 14{,}000$ the second-order coherence is oscillatory (Fig. 1C, top right panel), for the smaller photon number of $\bar{n} \cong 2100$ it exhibits biexponential behavior (Fig. 1C, top left panel), in good agreement with theory. The difference of damping constant and undamped oscillation frequency, as determined from the fits, is $(\delta - \omega_0)/2\pi = -99(7)$ MHz and 19(2) MHz for the two datasets, and consequently the data can be assumed to be in the oscillatory phase for the former and in the biexponential condensate phase for the latter dataset. The presence of both the thermal cloud and the condensate peak in the observed spectra (Fig. 1B), which are a consequence of Bose-Einstein (quantum) statistics, are attributed as evidence for the quantum many-body character of the phases.

Figure 2A schematically shows the hierarchy of phases for fixed values of the average photon and molecule number, and Fig. 2B gives a three-dimensional plot of the full expected phase diagram. The indicated crossover between lasing and condensation occurs when for $\kappa \gg \bar{M}_g B_{abs}$ the loss rate becomes so large that photons leak from the cavity before thermalizing via reabsorption (*27*, *28*). The phase transition between the intermediate oscillatory and the biexponential phases for $\delta = \omega_0$ occurs at $\sqrt{\kappa B_{em}\bar{n}} \simeq \frac{1}{2}B_{em}(\bar{M}_e/\bar{n} + \bar{n})$ and features a grand canonical $(\bar{M}_e \gg \bar{n}^2)$ and a canonical branch $(\bar{M}_e \ll \bar{n}^2)$ of the phase boundary, corresponding to the first or second term in the sum being dominant. Here, the first (grand canonical) term, understood to arise from retrapping of spontaneous emission, is absent in usual laser theory. Experimentally, with $\kappa/(\bar{M}_g B_{abs}) \cong 1.1 \times 10^{-3}$ photon thermalization dominates over photon loss, meaning that the exceptional point resides well inside the Bose-Einstein condensed regime.

To explore the phase transition between the two different condensate phases, we have recorded the photon number correlations at different average photon numbers. Figure 3A shows the variation of $\delta - \omega_0$, as determined from the fits of the correlation data. While for condensate sizes above $\bar{n}_{EP} \cong 2800$, the second-order coherence shows a damped oscillation, for smaller photon numbers, the data exhibits a biexponential decay of the correlations. Figure 3, B and C, shows the obtained decay times and, for the case of the oscillatory phase, the oscillation frequency depending on the condensate size. Both datasets give evidence for the photon condensate undergoing a non-Hermitian phase transition to the biexponential phase at a critical condensate occupation $\bar{n}_{EP}$. The deviation of the observed decay times from the prediction for short times is attributed to the 500-ps resolution of the detection system. Notably, when approaching the phase transition from below, the two characteristic decay times merge toward a single one, and when approaching the transition from above, the oscillation frequency converges to zero. This is in good agreement with the expectation that at the exceptional point, a (single) exponential decay of the second-order coherence occurs owing to the coalescence of the two eigenvalues, $\lambda_1 = \lambda_2 = \delta$. The revealed phase transition is visible in the temporal correlations but not in the average values.

Next, we recorded data at different cavity low-frequency cutoffs and dye concentrations, to explore the phase diagram beyond a single control parameter. The resulting change of the wavelength of condensate photons modifies both the loss as well as the Einstein coefficient. Because of the shape of the phase boundary at

$\delta = \omega_0$, upon rescaling the photon number as $\bar{n}/\sqrt{M_e}$ and the loss rate as $\kappa/B_{em}\sqrt{M_e}$, the phase diagram in Fig. 2B collapses to a two-dimensional one (*25*). Corresponding data are summarized in Fig. 4A. To obtain κ and the molecule number M, curves similar to those of a single dataset shown in Fig. 3 were fitted to all data. Our experimental data maps out the non-Hermitian phase transition between the oscillatory and biexponential phase within the investigated parameter range, in good agreement with expectations (black line). The variation of the normalized decay times and oscillation frequency versus the scaled loss rate in Fig. 4B for a fixed value of $n/\sqrt{M_e} \simeq 0.27$ demonstrate the branching of the eigenvalues when reducing the loss toward the idealized case of a perfect photon box.

The state of a macroscopic quantum system on different sides of an exceptional point can be in two distinct regimes. We have observed the associated dissipative phase transition from an oscillatory to a biexponential dynamical phase of a dye microcavity photon Bose-Einstein condensate and mapped out the corresponding phase diagram. This reveals a state of the light field, which, contrary to the usual picture of Bose-Einstein condensation, is separated by a phase transition from the phenomenon of lasing.

REFERENCES AND NOTES

1. M. A. Miri, A. Alù, *Science* **363**, eaar7709 (2019).
2. T. Fink, A. Schade, S. Höfling, C. Schneider, A. Imamoglu, *Nat. Phys.* **14**, 365–369 (2017).
3. G. Makey *et al*., *Nat. Phys.* **16**, 795–801 (2020).
4. N. Dogra *et al*., *Science* **366**, 1496–1499 (2019).
5. I. Prigogine, *Science* **201**, 777–785 (1978).
6. F. E. Öztürk *et al*., *Phys. Rev. A* **100**, 043803 (2019).
7. S. Diehl *et al*., *Nat. Phys.* **4**, 878–883 (2008).
8. R. Hanai, A. Edelman, Y. Ohashi, P. B. Littlewood, *Phys. Rev. Lett.* **122**, 185301 (2019).
9. K. Kawabata, K. Shiozaki, M. Ueda, M. Sato, *Phys. Rev. X* **9**, 041015 (2019).
10. E. Altman, L. M. Sieberer, L. Chen, S. Diehl, J. Toner, *Phys. Rev. X* **5**, 011017 (2015).
11. J. Klaers, J. Schmitt, F. Vewinger, M. Weitz, *Nature* **468**, 545–548 (2010).
12. Y. Sun *et al*., *Phys. Rev. Lett.* **118**, 016602 (2017).
13. I. Carusotto, C. Ciuti, *Rev. Mod. Phys.* **85**, 299–366 (2013).
14. J. Schmitt *et al*., *Phys. Rev. Lett.* **112**, 030401 (2014).
15. A. Griffin, D. W. Snoke, S. Stringari, Eds., *Bose-Einstein Condensation* (Cambridge Univ. Press, 1995).
16. B. T. Walker *et al*., *Nat. Commun.* **11**, 1390 (2020).
17. T. Kato, *Perturbation Theory of Linear Operators* (Springer, 1966).
18. C. M. Bender, S. Boettcher, *Phys. Rev. Lett.* **80**, 5243–5246 (1998).
19. T. Gao *et al*., *Nature* **526**, 554–558 (2015).
20. F. Minganti, A. Miranowicz, R. W. Chhajlany, F. Nori, *Phys. Rev. A* **100**, 062131 (2019).
21. W. D. Heiss, *J. Phys. A* **45**, 444016 (2012).
22. R. Hanai, P. B. Littlewood, *Phys. Rev. Res.* **2**, 033018 (2020).
23. J. Marelic, R. A. Nyman, *Phys. Rev. A* **91**, 033813 (2015).
24. S. Greveling, K. L. Perrier, D. van Oosten, *Phys. Rev. A* **98**, 013810 (2018).
25. See supplementary materials.
26. E. M. Kessler *et al*., *Phys. Rev. A* **86**, 012116 (2012).
27. P. Kirton, J. Keeling, *Phys. Rev. Lett.* **111**, 100404 (2013).
28. J. Schmitt *et al*., *Phys. Rev. A* **92**, 011602 (2015).
29. F. E. Öztürk *et al*., Observation of a non-Hermitian phase transition in an optical quantum gas, Version 1, Zenodo (2020); http://doi.org/10.5281/zenodo.4522437.

ACKNOWLEDGMENTS

We thank S. Diehl, M. Scully, and H. Stoof for discussions. **Funding:** We acknowledge support by the DFG, under SFB/TR 185 (277625399) and the Cluster of Excellence ML4Q (EXC 2004/1–390534769); the EU, under the Quantum Flagship project PhoQuS; and the DLR, with funds provided by the BMWi (50WM1859). J.S. thanks the University of Cambridge for support during the early stages of this work, and M.W. thanks the CAIQuE for providing a guest stay at UC Berkeley. **Author contributions:** F.E.Ö., T.L., J.S., and F.V. analyzed the data. J.S., J.Kl., and M.W. conceived of and designed the experiments. F.E.Ö., T.L., and J.Kr. contributed materials and/or analysis tools. F.E.Ö. and G.H. performed the experiments. F.E.Ö., T.L., J.S., F.V., J.Kr., and M.W. wrote the paper. **Competing interests:** The authors declare that they have no competing interests. **Data and materials availability:** Data shown in the figures are available in the Zenodo database (*29*).

SUPPLEMENTARY MATERIALS

science.sciencemag.org/content/372/6537/88/suppl/DC1
Materials and Methods
Supplementary Text
Table S1
References (*30*–*41*)

26 September 2020; accepted 23 February 2021
10.1126/science.abe9869

Observation of a non-Hermitian phase transition in an optical quantum gas

Fahri Emre Öztürk, Tim Lappe, Göran Hellmann, Julian Schmitt, Jan Klaers, Frank Vewinger, Johann Kroha and Martin Weitz

Science **372** (6537), 88-91.
DOI: 10.1126/science.abe9869

A dissipative quantum gas of light

Our textbook understanding of quantum systems tends to come from modeling these systems isolated from the environment. However, an emerging focus is understanding how many-body quantum systems behave when interacting with their surroundings and how they subsequently become dissipative, or non-Hermitian, systems. Öztürk *et al.* formed a quantum condensate of light by trapping photons in an optical cavity, a system that is naturally dissipative. By altering the trapping conditions, they demonstrated that the system provides a powerful platform with which to explore the complex dynamics and phase transitions occurring in dissipative quantum systems.

Science, this issue p. 88